Desalination and Water Treatment
www.deswater.com

doi: 10.5004/dwt.2018.22920

125 (2018) 61–67
September

Catalytic degradation of 4-chlorophenol by persulfate activated with magnetic $CuFe_2O_4$-Fe_3O_4 composite

Junhua Ma[a], Yong Liu[b,*], Xinglong Jin[a], Jianfei Bai[b]

[a]*College of Environment Science and Safety Engineering, Tianjin University of Technology, Tianjin 300384, China, Tel. +13132582052, email: majunhua19900512@163.com (M. Junhua), Tel. +13752636320, email: xljin7911@126.com (J. Xinlong)*
[b]*College of Chemistry and Chemical Engineering, Tianjin University of Technology, Tianjin 300384, China, Tel. +13920202859, 86 13920202859, email: tjutliuyong@163.com (Y. Liu), Tel. +13820269681, email: baijianfei1991@163.com (B. Jianfei)*

Received 330 September 2017; Accepted 5 August 2018

ABSTRACT

A novel heterogeneous $CuFe_2O_4$-Fe_3O_4 composite prepared in one pot was applied to activate persulfate for the degradation of 4-chlorophenol. The properties of $CuFe_2O_4$-Fe_3O_4 composite were characterized by the specific area (S_{BET}) measurement, X-ray diffraction (XRD), scanning electron microscopy (SEM) and Fourier-transform infrared spectra (FTIR). The experimental results showed that the catalytic performance of $CuFe_2O_4$-Fe_3O_4 is better than those of $CuFe_2O_4$ alone, Fe_3O_4 alone and the mixture ($CuFe_2O_4$/Fe_3O_4). The catalytic properties were investigated under different conditions (initial pH value, catalyst load, $Na_2S_2O_8$ dosage and 4-chlorophenol concentration). It was found that the removal of the 100 mg/L 4-chlorophenol achieved 96.35% after 120 min treatment with 2 g/L $Na_2S_2O_8$ when the initial pH value was 11. Under the same condition, total organic carbon (TOC) removal of 4-chlorophenol was 93.4% which demonstrated the degradation led to higher mineralization. Furthermore, the catalytic degradation mechanism was discussed. Cu(II), Fe(II) activated $Na_2S_2O_8$to form $SO_4^{\bullet-}$ and $^{\bullet}OH$ which was demonstrated by X-ray photo-electron spectroscopy (XPS) analysis and the quenching experiments.

Keywords: $CuFe_2O_4$-Fe_3O_4 composite; Persulfate; 4-CP; Radical mechanism

1. Introduction

Chlorophenols (CPs) are extremely toxic, poorly biodegradable, carcinogenic and recalcitrant [1]. Especially 4-chlorophenol (4-CP), a typical pollutant, was widely used as precursor for the synthesis of pesticides, herbicides, disinfectants and wood preservatives. Also chlorophenol was listed as one of the top priority pollutants by United States Environmental Protection Agency (USEPA) because it is irritant to the respiratory and central nervous systems at low levels, and can induce cancer at higher risks for the human health and caused serious damage to ecosystem [2,3]. It is urgent to develop efficient remedy approaches for the degradation of 4-CP in aqueous environment.

In recent years, advanced oxidation processes (AOPs) have been extensively applied for the degradation of CPs such as Fenton oxidation [4–6], O_3 oxidation [7], UV photolysis [8], photocatalytic [2], and persulfate (PS) oxidative degradation [9–11]. Among them, PS is a kind of strong and steady oxidation agent (E_0 = 2.01 V) with high solubility in water. It generates $SO_4^{\bullet-}$ as an in situ chemical oxidation (ISCO) with high oxidation potential (E_0 = 2.6 V) that is resemblance to $^{\bullet}OH$ (E_0 = 2.73 V) [12,13]. PS can be activated via heat [14,15], metallic ions (e.g., Fe^{2+}, Co^{2+} and Cu^{2+}) [4,7] as well as metallic oxides (Fe_3O_4, CuO and $CuFe_2O_4$) [12,16–18]. Thermal activation needs a large quantity of additional energy to make the water system meet the requested temperature, which highly raises the expense of water treatment. As for the PS activation by metallic ions, the metal leaching in water could not be completely ignored. Considering the leakage of metal ions caused exceed emission standard in the water and then brought about the other pollution. Therefore, much effort has been taken to develop an effective heterogeneous catalyst.

*Corresponding author.

Peroxymonosulfate (PMS) can be activated by $CuFe_2O_4$ which is served as an efficient catalyst in organic pollutants oxidation [19,20]. $CuFe_2O_4$ nanoparticles was also used to activate H_2O_2 for the removal of sulfanilamide and benzylic alcohols [21,22]. PS activated by $CuFe_2O_4$ decorated multi-walled carbon nanotubes magnetic nanoparticles was also used for the removal of diethyl phthalate [18]. Nevertheless PS activation mechanism by $CuFe_2O_4$ with other metal oxides composite has not been systematically explored. Iron with other metal oxides composite has attracted wide attention due to its excellent synergistic effect on organic pollutant degradation. Iron oxides precipitated on the surface of niobium oxide for the dye oxidation with H_2O_2 was more effective than iron oxides or niobium oxide alone [23]. CuO-Fe_3O_4 composite with PS has also used for the removal of phenol, which showed a better catalytic effect due to the reaction between iron and copper. Cu^{2+} generated the Cu^{3+} and then reacted with Fe^{2+} to regenerate Cu^{2+} which promoted the generation of radicals [17]. Magnetic nanoscale Fe_3O_4-CeO_2 composite, as an effective heterogeneous Fenton catalyst had good effect on oxidation of 4-chlorophenol due to the reaction of Fe^{2+} and Ce^{3+} with H_2O_2 [24]. However, the mechanism of iron oxides with $CuFe_2O_4$ has not been explored.

So far, there is no systematic study about the 4-CP removal by $CuFe_2O_4$-Fe_3O_4/PS available. And the mechanism of 4-CP degradation is confined. Therefore, this work focused on the oxidative degradation of 4-CP with $CuFe_2O_4$-Fe_3O_4/PS. The effect of $CuFe_2O_4$-Fe_3O_4/PS on the degradation of 4-CP has been proved. The influence factor of 4-CP concentration, $CuFe_2O_4$-Fe_3O_4 dosage, PS concentration and initial pH on the removal of 4-CP were also systematically investigated. Furthermore, the catalytic mechanism of $CuFe_2O_4$-Fe_3O_4/PS in 4-CP degradation was also proposed.

2. Material and methods

2.1. Chemicals

Chlorophenol (4-CP), ferrous sulfate heptahydrate ($FeSO_4{\cdot}7H_2O$), copper sulfate pentahydrate ($CuSO_4{\cdot}5H_2O$), hydrogen peroxide (H_2O_2, 30%), hydrochloric acid (HCl) Tween 20 ($C_{58}H_{114}O_{26}$), barium chloride dihydrate ($BaCl_2{\cdot}2H_2O$), sodium hydroxide (NaOH), sodium persulfate ($Na_2S_2O_8$), sodium sulfate anhydrous (Na_2SO_4), tertiary butyl alcohol ($C_4H_{10}O$), methanol (CH_3O) and ethanol absolute (C_2H_6O) were all obtained from Tianjin Concord Technology Company. Methanol was chromatographic reagent grade without further purification. The water used was Milli-Q water.

2.2. Preparation of $CuFe_2O_4$-Fe_3O_4

$CuFe_2O_4$-Fe_3O_4 was synthesized in one pot [5]. The mole ratio of Ferrous sulfate (11.12 g) and copper sulfate (1.0 g) was 10:1 and two materials were poured into a flask with three necks including 494 mL deionized water. And then 6 mL hydrogen peroxide (30%) was added using the peristaltic pump with 0.3 mL/min and stirred vigorously. After half an hour sodium hydroxide (0.5 mol/L) was added at 2 mL/min until the pH value reached in the range of 7–8. The suspension was stirred vigorously in water bath at 90°C for 1 h. After cooling down to the room temperature, the minerals were collected with qualitative filter paper. And then it was washed twice with hydrochloric acid (pH = 2), and three times with deionized water (pH = 6.8) to removal oxidized surfaces severally. At last, the collected metal composite was dried at 90°C for 6 h for the characterization and the following experiments .

2.3. Characterization of $CuFe_2O_4$-Fe_3O_4

The morphologies of $CuFe_2O_4$-Fe_3O_4 were characterized by ultrahigh-resolution scanning electron microscope with FEG (field emission (electron) gun). The $CuFe_2O_4$-Fe_3O_4 was characterized by X-ray diffraction (Rigaku Ultima IV) system in the 2θ range from 20° to 80°. The specific surface area of catalyst was identified by Brunauer–Emmett–Teller (BET, V-Sorb X800, Gold APP Instrument Corp). Fourier transform infrared spectra (FTIR, Nicolet 670, Thermo Fisher Scientific) was gathered on a Thermo Nicolet Nexus FTIR spectrometer by a KBr pressed disk method. X-ray photo-electron spectroscopy (XPS, Al K-Alpha, Thermo Fisher Scientific, USA) was used to confirm the chemical states both Cu and Fe.

2.4. Analysis

The concentration of 4-CP was measured determined via a high performance liquid chromatography (HPLC-6000PVW, CoMetro.) including follow equipments: a UV detection wavelength 278 nm as well as a Kromasil C_{18} separation column (250×4.6 mm, 5 μm). The mobile phase was 80:20 methanol and water at a flow of 1.0 mL/min. 20 μL test samples were injected under column temperature of 25°C. The aqueous Fe(II) and total dissolved Fe were measured at 510 nm by a colorimetric way via o-phenanthroline on a visible spectrophotometer (722, Jinghua). The concentrations of SO_4^{2-} was quantitative analyzed by $BaCl_2$ turbidi-metrical method. Total organic carbon (TOC) was determined by a TOC analyzer (TOC-5000, Shimadzu) to estimate the 4-CP mineralization.

2.5. Experiment

Experiments were conducted in a series of 250 mL conical bottles. The 4-CP and $CuFe_2O_4$-Fe_3O_4 were poured into the bottle. Then the initial pH value was measured by pH-meter (pH3210, WTW) and adjusted by hydrochloric acid (0.1 M) or sodium hydroxide (0.1 M) to the determined pH. All tests were carried out under the condition without light and the conical bottles shook with 180 rpm employing a WE-2 shaking bath (Honour Instrument Corp) at 25°C. Take out and then centrifuge 2 mL reaction sample at 12,000 rpm for 4 min after the determined reaction time. Filtered the supernatant liquid using a 0.45 μm Millipore filter before analyzing the 4-CP, dissolved iron, production of SO_4^{2-} and total organic carbon (TOC). All tests were performed in duplicate.

3. Results and discussion

3.1. Characterization of $CuFe_2O_4$-Fe_3O_4

The $CuFe_2O_4$-Fe_3O_4 composite morphology was characterized by SEM. As shown in Fig. 1, the nanoparticles were

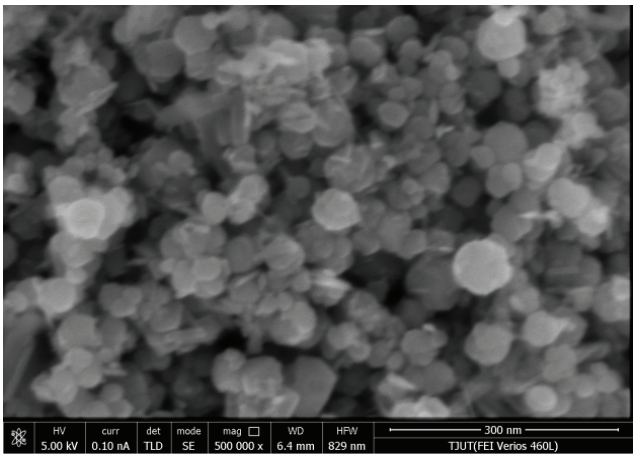

Fig. 1. SEM of $CuFe_2O_4$-Fe_3O_4.

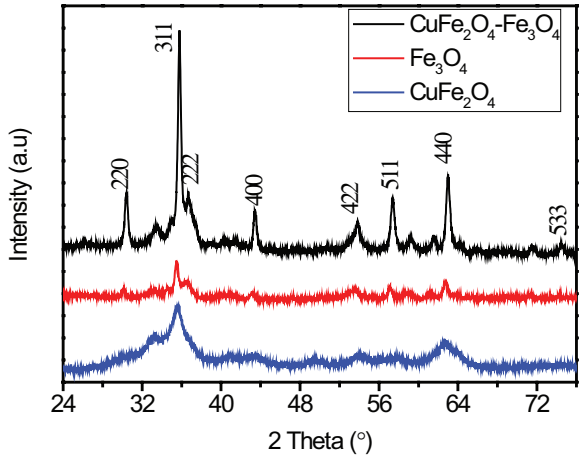

Fig. 2. XRD patterns of $CuFe_2O_4$-Fe_3O_4 and its two monomers.

homogeneous spherical shaped and tight arrangement with smaller agglomeration. It was obvious that the diameter of nanoparticle was below 80 nm. Furthermore, the synthetic $CuFe_2O_4$-Fe_3O_4 was characterized by XRD as shown in Fig. 2. The XRD patterns showed the diffraction peaks matched well with the published XRD pattern of the spherical $CuFe_2O_4$-Fe_3O_4 (JCPDS File No.25-0283 and 65-3107), indicating the formation with a quantity of crystallization. It was obvious that all peaks of $CuFe_2O_4$-Fe_3O_4 was more sharp than $CuFe_2O_4$ alone and Fe_3O_4 alone and the peak width at half height was more smaller so the composite had better crystallization. The composite also had more required material contents from the stronger peak compared to the $CuFe_2O_4$ and Fe_3O_4 peak superposition. N_2 adsorption-desorption isotherms (Table 1) structures of the catalysts. The BET surface area was 48.66 m^2/g and the average pore size of the catalyst was 24.87 nm. It was obvious larger than 4.88 m^2/g and 8.62 nm for CuO, 29.84 m^2/g and 15.14 nm for Fe_2O_3, indicating a large increase in the specific surface area of the $CuFe_2O_4$-Fe_3O_4 compared with CuO and Fe_2O_3 [19]. FTIR was an important tool to identify the stretching and bending vibrations of atoms on the surface of materials. It can be seen from Fig. 3 that the band at 3418 cm may be attributed to O-H stretching and band at1633 cm to the bending vibrations of H-O-H while those at 2350, 2025, 1106 and 1385 cm were gathered with their bending mode [25,26]. It also matched with stretching vibrations on the surface of metallic oxides at tetrahedral stretching M_{tetra}-O generally in the range 900–500 cm, while the other low band was often detected in the range of 450–350 cm designated to octahedral metal site M_{octa}-O [22,27]. $CuFe_2O_4$-Fe_3O_4 (a) was different from $CuFe_2O_4/Fe_3O_4$ (b) at 458 and 780 cm which made catalytic effect better.

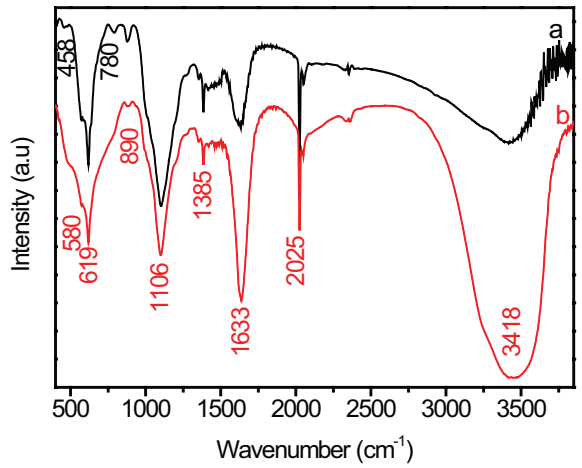

Fig. 3. FTIR of (a) $CuFe_2O_4$-Fe_3O_4 (b) $CuFe_2O_4/Fe_3O_4$.

3.2. Catalysts comparison experiments

A series of catalysts comparison experiments were conducted to comprehensively assess the catalytic efficiencies of 1 g/L $CuFe_2O_4$-Fe_3O_4, 0.22 g/L $CuFe_2O_4$ (the same $CuFe_2O_4$ dosage as $CuFe_2O_4$-Fe_3O_4), 0.78 g/L Fe_3O_4 (the same Fe_3O_4 dosage as $CuFe_2O_4$-Fe_3O_4), 1 g/L$CuFe_2O_4/Fe_3O_4$. Meanwhile, control experiments including $CuFe_2O_4$-Fe_3O_4 alone and PS alone were conducted before investigating the effectiveness of 4-CP degradation on PS activated by $CuFe_2O_4$-Fe_3O_4. As exhibited in Fig. 4, the degradation was observed less than 15% in $CuFe_2O_4$-Fe_3O_4 alone and PS alone indicating that the 4-CP potential losses by evaporation, adsorption and alkaline activated can be neglected during the system reaction. The degradation of PS activated by Fe_3O_4 was only 10.36% so Fe_3O_4 was not effective catalyst. The degradation of 4-CP was 96.35, 83.47 and 83.2 after 120 min under $CuFe_2O_4$-Fe_3O_4composite, $CuFe_2O_4$, $CuFe_2O_4/Fe_3O_4$ mixture respectively. $CuFe_2O_4$-Fe_3O_4 composite showed more effective than other catalysts suggesting that it has a synergy effect. $CuFe_2O_4$-Fe_3O_4 composite strengthened the relative speed by mass electrons transfer. It was similar to the transfer of electrons from $\equiv Fe^{2+}$ to $\equiv Ce^{4+}$ in magnetic nanoscale Fe_3O_4-CeO composite [24]. Moreover $CuFe_2O_4$-Fe_3O_4 composite had better crystallization and more required material contents compared to the mixture from the XRD. So the composite had better catalytic than mixture.

3.3. Factorial effects on 4-CP degradation

In this work 4-CP degradation under different conditions was carried out. For the $CuFe_2O_4$-Fe_3O_4/PS systems,

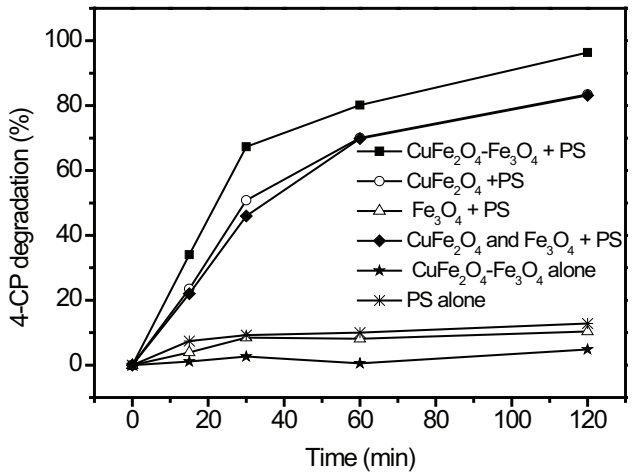

Fig. 4. Influence of control experimental and catalysts comparison on the removal of 4-CP. Experimental situations: $[4\text{-CP}]_0$ = 100 mg/L, $[Na_2S_2O_8]_0$ = 2 g/L and initial pH = 11.

catalyst dosage suggested a positive effect on the oxidative degradation of 4-CP. Four different catalysts load changing from 0.5 to 2.0 g/L were investigated. The reaction was carried out under 2 g/L PS, 100 mg/L 4-CP and constant temperature 25°C for 120 min. As shown in Fig. 5a, when the catalysts load was 0.5, 1.0, 1.5 and 2.0 g/L the degradation of 4-CP were 37.74%, 67.31%, 71.47% and 75.4% after 30 min treatment, respectively. An obvious increase from 0.5 to 1.0 g/L indicating that the degradation of the 4-CP was highly affected by a growing number of active sites but still unsaturated during the activated reaction for generation $SO_4^{\bullet-}$ used in degradation. While the more catalyst from 1.0 to 2.0 g/L did not make any obvious raising of the removal. It was indicated that excessive catalyst may enhance the decomposition of PS but lower utilization of $SO_4^{\bullet-}$ which ascribed to the radicals self-scavenging ability or scavenging with PS as Eqns. (1), (2) [12,28,29]. The degradation of 4-CP were 70.82%, 96.35%, 96.12% and 96.5% after 120 min, respectively. The degradation increased and achieved the desired effect at 1.0 g/L. Therefore in the present research, the optimum $CuFe_2O_4$-Fe_3O_4 dosage was 1.0 g/L for the following degradation experiments.

PS also plays key role of in the 4-CP degradation during the oxidation reaction. So, 4-CP degradation with four concentrations (1.0, 2.0, 3.0 and 4.0 g/L) of PS were studied in this work. The effects of PS concentration are shown in Fig. 5b. With 1.0, 2.0, 3.0 and 4.0 g/L PS, the degradation of 4-CP was 30.39%, 67.31%, 78.39% and 89.44% after 30 min treatment, respectively. When the treatment prolonged to 120 min, the degradation reached 57.83%, 96.35%, 96.27% and 96.19%, respectively. It was obvious that the degradation was improved with the increasing PS concentration which due to the enhancement of the PS activated by $CuFe_2O_4$-Fe_3O_4. It should be pointed out that 4-CP underwent partial degradation at 1.0 g/L due to less sulfate radicals ($SO_4^{\bullet-}$). The degradation of 4-CP improved with the increasing PS concentration attributing to the enhancement of the sulfate radicals generated. It was clear that the generation of more sulfate radicals resulted in the more rapid removal of 4-CP at higher PS dosage [30,31]. While the 4-CP degradation was not in proportion to the PS dosage, probably attributing to the quenching reaction of sulfate radicals by self-coupling reaction or residual PS reaction via Eqns. (1), (2).

$$SO_4^{\bullet-} + SO_4^{\bullet-} \rightarrow S_2O_8^{2-} \quad (1)$$

$$SO_4^{\bullet-} + S_2O_8^{2-} \rightarrow SO_4^{2-} + S_2O_8^{\bullet-} \quad (2)$$

The 4-CP concentration was essential for the degradation under the condition of determined PS and catalyst. The experiment at different 4-CP concentration was conducted with the 50, 100, 150 and 200 mg/L. The 4-CP was almost completely degraded after 30 min at 50 mg/L as seen in Fig. 5c. However it took 120 min when the 4-CP was 100mg/L. It was still less than 90% at initial 4-CP concentration 150 mg/L after longer time 240 min. For 4-CP at 200 mg/L it was only 80% under the condition as above. The degrading effect decreased with the increasing 4-CP concentration. Higher initial 4-CP concentration would lead to the increase of $SO_4^{\bullet-}$ and $^{\bullet}OH$ decomposition but without enough radicals for high concentration of 4-CP resulted in a little low removal.

The catalytic removal process of 4-CP was largely influenced by the pH value of solution. The pH influence of the 4-CP degradation the experiment at different initial pH was conducted with the initial pH as 3, 5, 7, 9, 10, 11 and 12. As shown in Fig. 5d, the degradation efficiency was less than 20% under pH 3, 5, 7 and 9 and largely enhanced from pH 10 to 12. It was only 60.6% at pH 10 and can be further improved to 96.35% at pH 11 after 120 min and to 96.4% at pH 12 after 30 min. So the most optimum pH was at pH 11 for other experiment considering the degradation effect and practical application. The pH cut down with follow reaction time and at last maintained relatively stable values pH 7 after 30 min. And it was degraded about 70% after 30 min. It was also tested that the degradation reached 98.3% after 15 min treatment when pH retained at 11. It might be advantageous at high pH condition for regenerating hydroxyl groups on the surface of $CuFe_2O_4$-Fe_3O_4 composite surface as an active site for electron transfer beneficially agreed with Lei [17]. The reaction occurred on the surface instead of metal ions in the solution so it was more effective in alkaline environment than acid due to the dissolution of $CuFe_2O_4$-Fe_3O_4 composite in acid. Also it was good for generate of $^{\bullet}OH$ in alkaline than acid environment.

3.4. Degradation products and pathways

To measure the mineralization of 4-CP in the $CuFe_2O_4$-Fe_3O_4/PS system, the TOC degradation value is calculated in the report defined as Eq. (3) :

$$TOC_{removal} = \frac{TOC_0 - TOC_t}{TOC_0} \times 100\% \quad (3)$$

where TOC_t and TOC_0 are the TOC ratios at reaction time t and 0 apart [32]. The TOC of the 4-CP solution was 93.4% after 120 min treatment approximately equal to the 4-CP removal which showed that most 4-CP was degraded into organic intermediates then almost absolutely oxidized into CO_2 and H_2O.

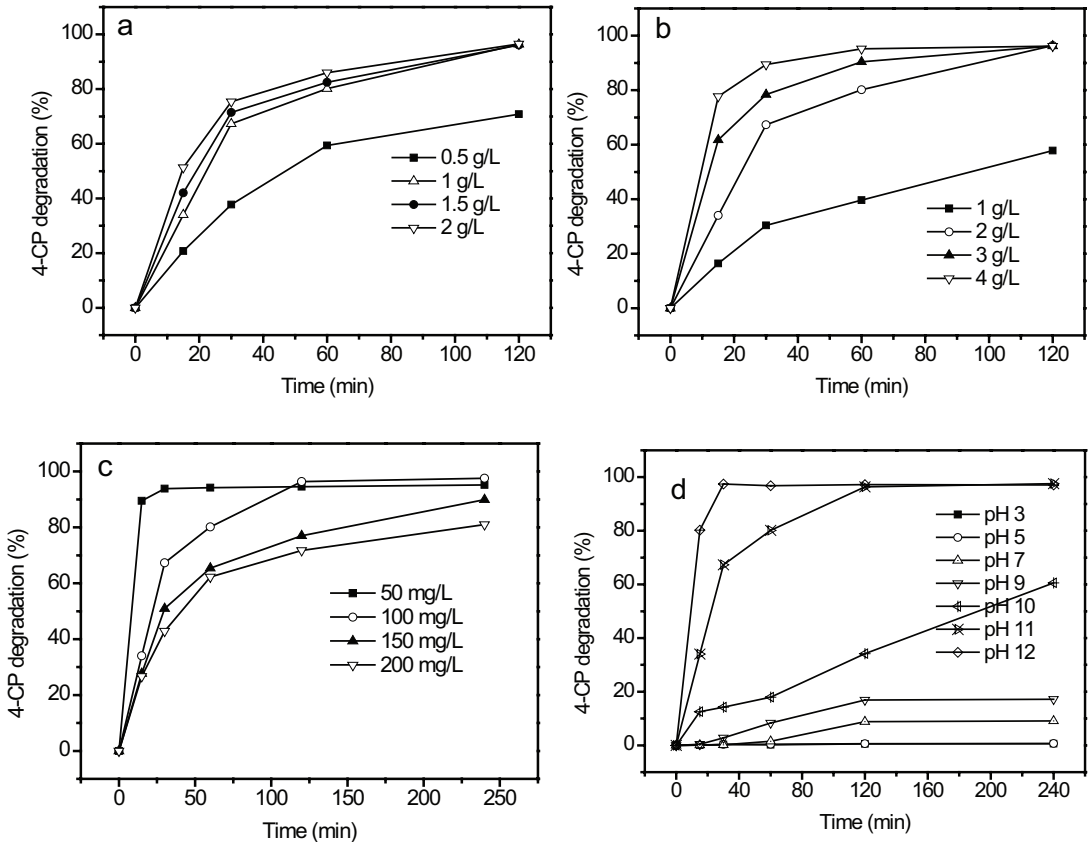

Fig. 5. Factorial effects on removal of 4-CP: (a) catalyst dosage (b) PS dosage (c) 4-CP concentration (d) initial pH. Except for the researched parameter, other parameters were certain: $[CuFe_2O_4\text{-}Fe_3O_4]_0$ = 1 g/L, $[4\text{-CP}]_0$ = 100 mg/L, $[Na_2S_2O_8]_0$ = 2 g/L and initial pH = 11.

3.5 The catalytic mechanism of $CuFe_2O_4$-Fe_3O_4

For purpose of the mechanism of 4-CP removal, different quenching agent including methanol and tertiary butanol was selected as an efficient radical scavengers to distinguish the radicals type [33]. Methanol was used to quench both $SO_4^{\bullet-}$ (1.6×10^7–7.7×10^7 M^{-1} S^{-1}) and $^{\bullet}OH$ (1.2×10^9–2.8×10^9 M^{-1} S^{-1}) while tertiary butanol was applied to quench $^{\bullet}OH$ (3.8×10^8–7.6×10^8 M^{-1} S^{-1}) approximately 1000 times larger than that with $SO_4^{\bullet-}$ (4×10^5–9.1×10^5 M^{-1} S^{-1}) [34]. Hence methanol was used to scavenge both radicals, and tertiary butanol was used to quench $^{\bullet}OH$ merely. Fig. 6 showed that under the condition of methanol the removal of 4-CP was highly declined but less in the tertiary butanol, which indicated supplements a focus on $SO_4^{\bullet-}$ with $^{\bullet}OH$ during the reaction. When 20% methanol, 20% tertiary butanol (volume fraction) were added, the degradation decreased to 63.8% and 24.3% in the degradation of catalytic oxidation, respectively. It was no 4-CP degradation with the 20% methanol and 20% tertiary butanol. Thus, it is a conclusion that $SO_4^{\bullet-}$ plays an essential role with the assistance of $^{\bullet}OH$ in the $CuFe_2O_4$-Fe_3O_4/PS system.

For a better understanding of the surface decomposition and chemical species of the $CuFe_2O_4$-Fe_3O_4 composite before and after the removal process, and the key parts of the Cu and Fe states and radical groups during the activation period of PS, XPS spectra of $CuFe_2O_4$-Fe_3O_4 before and after reaction are compared in Fig. 7. Considering the fresh catalyst, the high-resolution spectra of the peaks at 710.8 eV and 712.7 eV are indicative of the presence of Fe(II) and Fe(III). For the XPS spectra of Cu $2p_{3/2}$ region, the main peak at binding energy of 933.8 and 934.2 eV is assigned

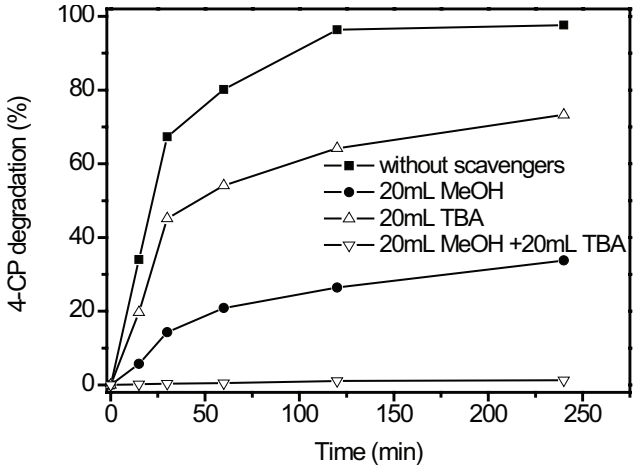

Fig. 6. Influence of different quenching agent on the removal of 4-CP. Experimental conditions: initial pH = 11, $[CuFe_2O_4\text{-}Fe_3O_4]_0$ = 1 g/L, $[Na_2S_2O_8]_0$ = 2 g/L and $[4\text{-CP}]_0$ = 100 mg/L.

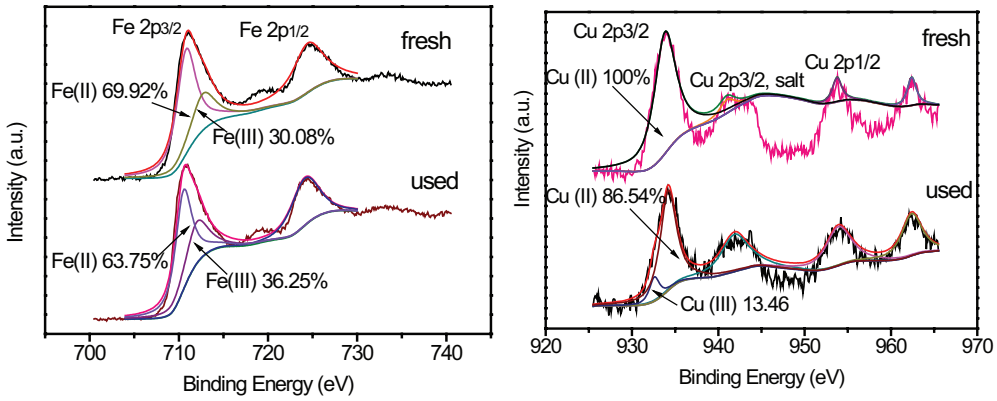

Fig. 7. XPS spectra for Fe 2p regions and Cu 2p regions of fresh and used $CuFe_2O_4$-Fe_3O_4.

to Cu(II) and 932.6 eV to Cu(III). After reaction, the proportion of Fe(II) status decreased from 69.92% to 63.75%, indicating the oxidation of Fe(II) into Fe(III) status. The proportion of Cu(II) decreased from 100% to 86.54%, indicating the oxidation of Cu(II) into Cu(III) status. This is probably due to the reaction among Fe(II) and PS at the same time the redox reaction between Cu(III) and Fe(II) via Eq. (8). The dosage of ion leaching and SO_4^{2-} production were measured, the consequence are suggested in Fig. 8. The iron ions dosage initially raised in the reaction because aqueous Fe(II) was gradually released into the reaction systems from the $CuFe_2O_4$-Fe_3O_4 surface with the substantial decomposition of PS to form $SO_4^{\bullet-}$ and $^{\bullet}OH$. It was clear that ion leaching can be essentially ignored less than 1 mg/L which confirmed the catalytic reaction on the $CuFe_2O_4$-Fe_3O_4surface. The concentration of SO_4^{2-} increased from 0 to 320 mg/L in 15 min, which indicated that much faster removal of 4-CP.

On the basis of all the results obtained above, a possible mechanism for PS activated by $CuFe_2O_4$-Fe_3O_4 is put forward. Firstly a Fenton-like reaction occurred between Cu(II) and PS or Fe(II) and PS at the surface of $CuFe_2O_4$-Fe_3O_4 gathered with the generation of Cu(III), Fe(III), SO_4^{2-} and $SO_4^{\bullet-}$as Eqns. (4)–(7) which may lead to the formation of $^{\bullet}OH$ radicals as Eq. (9). Particularly the reproduce of Cu(II) by Fe(II) promotes the continuous decomposition of PS and the generate of radicals at the surface of $CuFe_2O_4$-Fe_3O_4. At the same time, the suface-adsorbed radicals might diffuse into the reaction system. The whole radicals account for the destruction of 4-CP.

$$\equiv Cu(II) + S_2O_8^{2-} \rightarrow \equiv Cu(II) \cdots O_3SO_2SO_3^{2-} \quad (4)$$

$$\equiv Cu(II) \cdots O_3SO_2SO_3^{2-} \rightarrow \equiv Cu(III) + SO_4^{\bullet-} + SO_4^{2-} \quad (5)$$

$$\equiv Cu(III) + H_2O \rightarrow \equiv Cu(II) + {}^{\bullet}OH + H^+ \quad (6)$$

$$\equiv Fe(II) + S_2O_8^{2-} \rightarrow \equiv Fe(III) + SO_4^{\bullet-} + SO_4^{2-} \quad (7)$$

$$\equiv Cu(III) + \equiv Fe(II) \rightarrow \equiv Fe(III) + \equiv Cu(II) \quad (8)$$

$$SO_4^{\bullet-} + OH^- \rightarrow +SO_4^{2-} + {}^{\bullet}OH \quad (9)$$

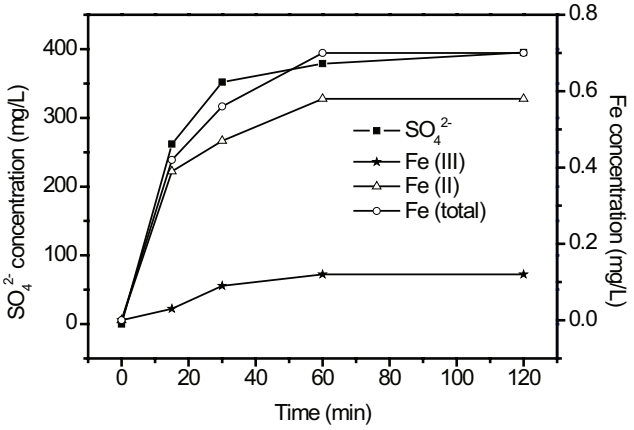

Fig. 8. The dosage of iron ion and SO_4^{2-} concentration on the removal of 4-CP. Experimental situations: initial pH = 11, $[CuFe_2O_4\text{-}Fe_3O_4]_0$ = 1 g/L, $[Na_2S_2O_8]_0$ = 2 g/L and $[4\text{-CP}]_0$ = 100 mg/L.

Table 1
BET Specific surface area, pore size and total pore volume of $CuFe_2O_4$-Fe_3O_4

Catalyst	$CuFe_2O_4$-Fe_3O_4
Specific surface area (m^2/g)	48.66
Pore size (nm)	24.87
Pore volume (m^3/g)	0.002158

4. Conclusions

A novel $CuFe_2O_4$-Fe_3O_4, prepared in one pot, was applied to activate persulfate for the degradation of 4-CP. The synthetic composite was effective to decompose PS to generate a great number of $SO_4^{\bullet-}$ with $^{\bullet}OH$ for the degradation of 4-CP. The degradation was 96.35 after 120 min. The $CuFe_2O_4$-Fe_3O_4/PS system by the 93.4% of TOC removal after 120 min was evidence suggesting the practicability of mineralization of 4-CP. At last it had a negative impact on 4-CP degradation in the presence of quenching agents including methanol and tertiary butanol. It was

found that the 4-CP mineralization by $CuFe_2O_4$-Fe_3O_4 catalyzed removal on the basis of radicals-type mechanism that $SO_4^{\bullet-}$ plays a dominant role with the assistance of •OH. Especially the reproduce of Cu(II) by Fe(II) favors the continuous decomposition of PS and at the same time with the generation of radicals at the surface of $CuFe_2O_4$-Fe_3O_4 composite. Cu(II) and PS generated Cu(III) at the surface of $CuFe_2O_4$-Fe_3O_4 which promoted the reaction system cycle and showed good synergy.

Acknowledgments

This study was supported by the National Natural Science Foundation of China (Grant No. 41201487).

References

[1] S. Sharma, M. Mukhopadhyay, Z.V.P. Murthy, Degradation of 4-chlorophenol in wastewater by organic oxidants, Ind. Eng. Chem. Res., 49 (2010) 3094–3098.
[2] G. Huang, S. Zhang, T. Xu, Y. Zhu, Fluorination of $ZnWO_4$ photocatalyst and influence on the degradation mechanism for 4-chlorophenol, Environ. Sci. Technol., 42 (2008) 8516–8521.
[3] W. Shen, Y. Mu, B. Wang, Z. Ai, L. Zhang, Enhanced aerobic degradation of 4-chlorophenol with iron-nickel nanoparticles, Appl. Surf. Sci., 393 (2017) 316–324.
[4] M. Barreto-Rodrigues, J. Silveira, P. García-Muñoz, J. Rodriguez, Dechlorination and oxidative degradation of 4-chlorophenol with nanostructured iron-silver alginate beads, J. Environ. Chem. Eng., 5 (2017) 838–842.
[5] M. Wang, G. Fang, P. Liu, D. Zhou, C. Ma, D. Zhang, J. Zhan, Fe_3O_4@β-CD nanocomposite as heterogeneous Fenton-like catalyst for enhanced degradation of 4-chlorophenol (4-CP), Appl. Catal. B Environ., 188 (2016) 113–122.
[6] Z. Ai, Z. Gao, L. Zhang, W. He, J. Yin, Core-shell structure dependent reactivity of Fe@Fe_2O_3 nanowires on aerobic degradation of 4-chlorophenol, Environ. Sci. Technol., 47 (2013) 5344–5352.
[7] W. Ma, P. Zong, Z. Cheng, B. Wang, Q. Sun, Adsorption and bio-sorption of nickel ions and reuse for 2-chlorophenol catalytic ozonation oxidation degradation from water, J. Hazard. Mater., 266 (2014) 19–25.
[8] J. Yuan, Q. Wu, P. Zhang, J. Yao, T. He, Y. Cao, Synthesis of indium borate and its application in photodegradation of 4-chlorophenol, Environ. Sci. Technol., 46 (2012) 2330–2336.
[9] Y. Guo, Z. Zeng, Y. Li, Z. Huang, J. Yang, Catalytic oxidation of 4-chlorophenol on in-situ sulfur-doped activated carbon with sulfate radicals, Sep. Purif. Technol., 179 (2017) 257–264.
[10] H. Chen, Z. Zhang, M. Feng, W. Liu, W. Wang, Q. Yang, Y. Hua, Degradation of 2,4-dichlorophenoxyacetic acid in water by persulfate activated with FeS (mackinawite), Chem. Eng. J., 313 (2017) 498–507.
[11] X. Li, M. Zhou, Y. Pan, L. Xu, Pre-magnetized Fe^0/persulfate for notably enhanced degradation and dechlorination of 2,4-dichlorophenol, Chem. Eng. J., 307 (2017) 1092–1104.
[12] Y. Leng, W. Guo, X. Shi, Y. Li, L. Xing, Polyhydroquinone-coated Fe_3O_4 nanocatalyst for degradation of Rhodamine B based on sulfate radicals, Ind. Eng. Chem. Res., 52 (2013) 13607–13612.
[13] C. Luo, J. Ma, J. Jiang, Y. Liu, Y. Song, Y. Yang, Y. Guan, D. Wu, Simulation and comparative study on the oxidation kinetics of atrazine by UV/H_2O_2, UV=HSO_5^- and UV=$S_2O_8^{2-}$, Water Res., 80 (2015) 99–108.
[14] X. Xie, Y. Zhang, W. Huang, S. Huang, Degradation kinetics and mechanism of aniline by heat-assisted persulfate oxidation, J. Environ. Sci., 24 (2012) 821–826.
[15] M. Nie, Y. Yang, Z. Zhang, C. Yan, X. Wang, H. Li, W. Dong, Degradation of chloramphenicol by thermally activated persulfate in aqueous solution, Chem. Eng. J., 246 (2014) 373–382.
[16] Y. Leng, W. Guo, X. Shi, Y. Li, A. Wang, F. Hao, L. Xing, Degradation of Rhodamine B by persulfate activated with Fe_3O_4: Effect of polyhydroquinone serving as an electron shuttle, Chem. Eng. J., 240 (2014) 338–343.
[17] Y. Lei, C. Chen, Y. Tu, Y. Huang, H. Zhang, Heterogeneous degradation of organic pollutants by persulfate activated by CuO-Fe_3O_4: Mechanism, stability, and effects of pH and bicarbonate ions, Environ. Sci. Technol., 49 (2015) 6838–6845.
[18] X. Zhang, M. Feng, R. Qu, H. Liu, L. Wang, Z. Wang, Catalytic degradation of diethyl phthalate in aqueous solution by persulfate activated with nano-scaled magnetic $CuFe_2O_4$/MWCNTs, Chem. Eng. J., 301 (2016) 1–11.
[19] Y. Xu, J. Ai, H. Zhang, The mechanism of degradation of bisphenol A using the magnetically separable $CuFe_2O_4$/peroxymonosulfate heterogeneous oxidation process, J. Hazard. Mater., 309 (2016) 87–96.
[20] X. Zhang, M. Feng, L. Wang, R. Qu, Z. Wang, Catalytic degradation of 2-phenylbenzimidazole-5-sulfonic acid by peroxymonosulfate activated with nitrogen and sulfur co-doped CNTs-COOH loaded $CuFe_2O_4$, Chem. Eng. J., 307 (2017) 95–104.
[21] Y. Feng, C. Liao, K. Shih, Copper-promoted circumneutral activation of H_2O_2 by magnetic $CuFe_2O_4$ spinel nanoparticles: Mechanism, stoichiometric efficiency, and pathway of degrading sulfanilamide, Chemosphere, 154 (2016) 573–582.
[22] A. Manikandan, M. Durka, S. Arul Antony, Hibiscus rosa-sinensis leaf extracted green methods, magneto-optical and catalytic properties of spinel $CuFe_2O_4$ nano- and microstructures, J. Inorg. Organomet. Polym., 3 (2015) 14.
[23] L.C.A. Oliveira, M. Goncalves, M.C. Guerreiro, T.C. Ramalho, J.D. Fabris, M.C. Pereira, K. Sapag, A new catalyst material based on niobia/iron oxide composite on the oxidation of organic contaminants in water via heterogeneous fenton mechanisms, Appl. Catal. A Gen., 316 (2007) 117–124.
[24] L. Xu, J. Wang, Magnetic nanoscaled Fe_3O_4/CeO_2 composite as an efficient Fenton-like heterogeneous catalyst for degradation of 4-chlorophenol, Environ. Sci. Technol., 46 (2012) 10145–10153.
[25] A. Manikandan, E. Hema, M. Durka, K. Seevakan, T. Alagesan, S. Arul Antony, Room temperature ferromagnetism of magnetically recyclable photocatalyst of $Cu_{1-x}Mn_xFe_2O_4$-TiO_2 ($0.0 \le x \le 0.5$) nanocomposites, J. Supercond. Nov. Magn., 28 (2015) 1783–1795.
[26] D. Wan, G. Wang, W. Li, X. Wei, Investigation into the morphology and structure of magnetic bentonite nanocomposites with their catalytic activity, Appl. Surf. Sci., 413 (2017) 398–407.
[27] S. Sehatia, M.H. Entezari, Sono-incorporation of CuO nanoparticles on the surface and into the mesoporous hexatitanate layers: Enhanced Fenton-like activity in degradation of orange-G at its neutral pH, Appl. Surf. Sci., 399 (2017) 732–741.
[28] Y. Ding, L. Zhu, N. Wang, H. Tang, Sulfate radicals induced degradation of tetrabromobisphenol A with nanoscaled magnetic $CuFe_2O_4$ as a heterogeneous catalyst of peroxymonosulfate, Appl. Catal. B Environ., 129 (2013) 153–162.
[29] Y. Zhang, Q. Zhang, J. Hong, Sulfate radical degradation of acetaminophen by novel iron-copper bimetallic oxidation catalyzed by persulfate: Mechanism and degradation pathways, Appl. Surf. Sci., 422 (2017) 443–451.
[30] R.E. Huie, C.L. Clifton, Rate constants for hydrogen abstraction reactions of the sulfate radical, $SO_4^{-\bullet}$ alkanes and ethers, Int. J. Chem. Kinet., 21 (1989) 611–619.
[31] A. Seid-Mohammadi, A. Shabanloo, M. Fazlzadeh, Y. Poureshgh, Degradation of Acid Blue 113 by US/H_2O_2/Fe^{2+} and US/$S_2O_8^{2-}$/Fe^{2+} processes from aqueous solutions, Desal. Wat. Treat., 78 (2017) 273–280.
[32] H. Duan, Y. Liu, X. Yin, J. Bai, J. Qi, Degradation of nitrobenzene by Fenton-like reaction in a H_2O_2/schwertmannite system, Chem. Eng. J., 283 (2016) 873–879.
[33] J. Li, P. Ye, J. Fang, M. Wang, D. Wu, A. Xua, X. Li, Peroxymonosulfate activation and pollutants degradation over highly dispersed CuO in manganese oxide octahedral molecular sieve, Appl. Surf. Sci., 422 (2017) 754–762.
[34] S. Yang, X. Yang, X. Shao, R. Niu, L. Wang, Activated carbon catalyzed persulfate oxidation of Azo dye acid orange 7 at ambient temperature, J. Hazard. Mater., 186 (2011) 659–666.